Journal of The Electrochemical Society, **152** (12) C817-C826 (2005)
0013-4651/2005/152(12)/C817/10/$7.00 © The Electrochemical Society, Inc.

Electrochemical Deposition of Co under the Influence of High Magnetic Fields

M. Uhlemann,[a,z] A. Krause,[a] J. P. Chopart,[b] and A. Gebert[a]

[a] *Leibniz-Institute for Solid State and Materials Research, IFW-Dresden, 01171 Dresden, Germany*
[b] *DTI, EA 3083, UFR Sciences, 51687 Reims Cedex 2, France*

The effect of uniform, vertically oriented high magnetic fields up to 13 T on the electrodeposition of Co has been investigated in dependence on the cell and electrode geometry as well as the orientation and strength of the magnetic flux density by means of cyclic voltammetry, chronoamperometric measurements, and atomic force microscopy investigations. In the majority of cases, the limiting current density i_{lim} increases with increasing magnetic flux densities independent of the cell geometry and orientation. The current efficiency of Co increases with increasing magnetic flux densities only in magnetic fields aligned parallel to the electrodes due to the magnetohydrodynamic (MHD) effect. The morphology of the deposits exhibits randomly oriented round-shaped grains. The electrochemical behavior of horizontal electrodes with magnetic fields oriented perpendicular to the surface is strongly dependent on the electrode geometry. The current efficiency of the Co deposition on flat electrodes increases for low magnetic flux densities and keeps constant for high magnetic fields. In contrast, for wall electrodes the current efficiency decreases strongly even for low magnetic fields. These results are caused by overlapping effects of two types of convection, macro-MHD- and micro-magneto convection due to gradients of the concentration and the magnetic susceptibility. This leads to a modified morphology.
[DOI: 10.1149/1.2073167]

Manuscript submitted March 31, 2005; revised manuscript received June 8, 2005. Available electronically October 24, 2005.

Magnetic field effects on electrochemical reactions and in particular on the deposition of metals are widely accepted and summarized in reviews of Fahidy[1,2] and Taken.[3] Proved and established are the convective magnetohydrodynamic effects (MHD) generated by the magnetic field acting on the mass transport and their consequence for the morphology of the deposits. Generally, hydrodynamic electrodes and convective effects are extensively investigated and semiempirically analyzed based on the fundamental equations of Navier–Stokes and the convective diffusion equations. A laminar flow close to the electrode surface increases the mass-transport rate and therefore, the limiting current (I_{lim}) is enhanced as soon as an inhibiting species is not favored by the magneto-induced convection.[4,5] According to the basic investigations discussed in Ref. 6, I_{lim} is dependent on the flow rate in the vicinity of the electrode. For stationary disk electrodes the following approximations based on the transport equations were obtained for a uniform laminar or rotating flow of the electrolyte

$$I_{\text{lim}} = knFc_{\infty}D^{2/3}\nu^{-1/6}\frac{\pi}{4}d^2(u/d)^{1/2} \qquad [1]$$

$$I_{\text{lim}} = knFc_{\infty}D^{2/3}\nu^{-1/6}\frac{\pi}{4}d^2\omega^{1/2} \qquad [2]$$

where k is 0.753–0.780, n is the number of electrons, c is the electroactive species concentration in the bulk electrolyte, D is the diffusion coefficient, $\nu = 10^{-6}$ m^2/s is the kinematic viscosity, F is the Faraday constant, d is the diameter of the disk electrode, u is the laminar velocity, and ω is the rotating velocity of the solution close to the electrode. First Aogaki et al.[7,8] investigated and quantified the convective effect of an applied magnetic field oriented parallel to the electrode surface on the limiting current density for the electrodeposition of Cu. From the experimental data and the analysis of the basic transport equations (Eq. 1 and 2) it has been found that the limiting current density (i_{lim}) is proportional to $c_{\infty}^{4/3}$ and B^b. The exponential dependency of i_{lim} from c_{∞} and B is widely established and proved by numerous groups.[9-12] The exponent b varies between 0.3 and 0.5, depending on the cell and electrode geometry and on the electroactive species in the solution. Aaboubi et al.[9] introduced a velocity gradient $\alpha = kBc_{\infty}$ for steady-state conditions and found the following relation considering the velocity gradient to be constant

$$i_{\text{lim}} = 0.687nFc_{\infty}D^{2/3}d^{5/3}\alpha^{1/3} \qquad [3]$$

Hence, it can be concluded from this relation (Eq. 3) and Eq. 1 and 2, that $i_{\text{lim}} \propto B^{1/3} \propto u^{1/2}$ or $\omega^{1/2}$. Therefore, the velocity at the interface diffusion layer/bulk electrolyte should be proportional to $B^{2/3}$. Based on the semiquantitative solution of hydrodynamic equations and the known magnetically induced convection, some authors[13-15] found a dependency of i_{lim} on the number of electrons involved in the electrochemical mass-transport-controlled process under the effect of external magnetic fields on stationary disk millielectrodes.

The theory of the hydrodynamic electrodes assumes that the diffusion layer is not moved and the transport of the electroactive species is only controlled by the diffusion. Therefore, mechanical stirring or magnetically induced convection takes place only outside of the diffusion layer. A convective flow inside the diffusion layer of electrodes with magnetic fields parallel to the surface is proposed by Olivier et al.[16] This motion is attributed to electrokinetic effects caused by the tangential component of the electric field and is not necessarily related to the presence of a magnetic field.[17] Especially the assumption that the motion of ions inside the double layer is only determined by diffusion is not sustainable for systems with magnetic fields oriented perpendicular to the surface. Additional fluid motions have also been predicted for these electrode configurations. Until now only a few studies are published for this case and the results are still controversial. With respect to this magnetic field configuration, Aogaki et al.[18-20] analyzed symmetrical and nonsymmetrical fluctuations forming micro- and macroscopic vortexes which yield characteristic morphologies consisting of regular microholes. In the magnetic field the macroscopic fluctuations are attributed to local breaks of the electrostatic equilibrium in the electric double layer, and the microvortexes are generated by the thermal motion inside the diffusion layer. This assumption predicts that the surface has an effect on the nucleation process during the deposition in an applied magnetic field. Recently, investigations of the authors[21,22] regarding the deposition of Co have shown that for the configuration of B perpendicular to the electrode surface the magnetic field increases i_{lim} but decreases the current efficiency for the Co deposition. High-magnetic-field investigations of the Cu deposition refer to an oscillating behavior of i_{lim}.[23] This behavior could be caused by the Lorentz force generating a rotating flow at the edge of the electrode due to nonparallel electric field lines. The motion of the ions at the vicinity of the surface could also be affected by other magnetically induced forces. For ions with high magnetic susceptibilities the interaction of the external field with the magnetic properties of the ions can lead to an additional driving force toward, or away from, the electrode, depending on the magnetic properties of

[z] E-mail: m.uhlemann@ifw-dresden.de

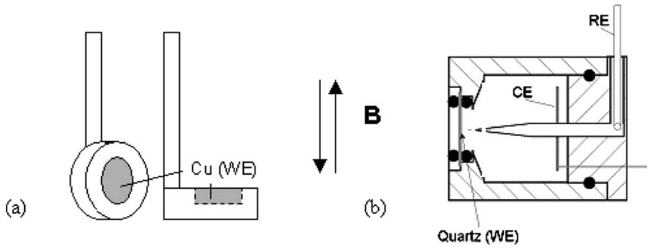

Figure 1. Electrochemical cells: (a) embedded Cu disk ($d = 11.3$ mm) arranged in a glass cylinder; (b) quartz crystal ($d = 14.05$ mm) fixed with O-rings forming a wall in a Teflon cell. The cells are placed horizontally and vertically in a vertical magnetic field.

the electroactive species and on the concentration gradient in the electrochemical double layer. This paramagnetic gradient force

$$F_{\nabla p} = \chi \frac{B^2}{2\mu_0} \nabla c \qquad [4]$$

was discussed by O'Brien and Santhanam,[24,25] Waskaas and Kharkats,[26,27] and Bund et al.[28] for different electrochemical systems and cell geometries. This gradient force has a short range and thus acts only near the electrode. Besides that, the magnetic field gradient force, caused by nonhomogeneous magnetic fields or induced by ferromagnetic substrates, can sufficiently influence the transport of paramagnetic or diamagnetic active species

$$F_{\nabla B} = \chi \frac{B \nabla B}{\mu_0} c \qquad [5]$$

The parameter μ_0 is the magnetic permeability and χ is the magnetic susceptibility of the elecroactive species. This force can be effective in the whole volume as well as close to the electrode for ferromagnetic substrates. White et al.[29-32] investigated this magnetic gradient force generated in nonhomogeneous fields on microelectrodes. The magnitude of the different magnetically induced forces and the influence on the fluid motion were estimated by Hinds et al.[33] Recently, Sugiyama et al.[34,35] have visualized and quantitatively examined that heterogeneous convection takes place on microdisk electrodes in nonuniform vertical magnetic fields. It has been concluded that the current density is controlled by magnetoconvection and is proportional to the power of one third of the magnetic flux density and its gradient as well as of the gradient of the magnetic susceptibility. For paramagnetic systems under unstable conditions the average current density has been derived to

$$i = 0.0969 nFc_{\infty} D \left(\frac{1}{\mu_0 D\eta}\right)^{1/3} \left(\frac{\partial \chi}{\partial c}\right)^{1/3} |\Delta c|^{4/3} \left| B \left(\frac{dB}{dz}\right)_{z=0} \right|^{1/3} \qquad [6]$$

With increasing radius of the disk electrode the diffusion current is increasingly determined by MHD convection, inducing a rotating flow. Therefore, for systems with high gradients of concentration and magnetic susceptibilities, respectively, and gradients of magnetic flux density, both phenomena, the magnetoconvection and the MHD effect, overlap and have to be taken into account.

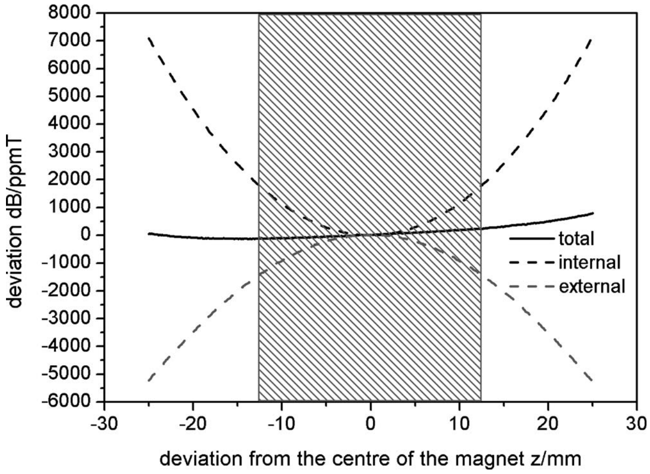

Figure 2. Homogeneity of the magnetic flux density in dependence on the distance z from the center of the magnet (Ref. 36); the diagonal pattern shows the size of the Teflon cell (Fig. 1b).

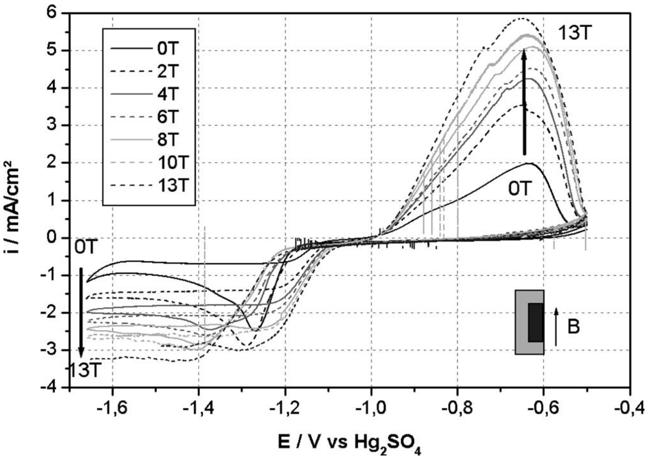

Figure 3. Cyclic voltammograms recorded in 0.01 M $CoSO_4$ + 0.1 M Na_2SO_4, pH 3, on flat embedded vertical Cu electrodes for different magnetic flux densities; B is aligned upward, $dE/dt = 20$ mV/s, 3rd scan.

First, results are presented regarding the effect of uniform high magnetic fields on the electrodeposition of Co in dependence on the cell and electrode geometry, the orientation, and the strength of the magnetic flux density. The change of i_{lim} and of the current efficiency as well as the effect of the magnetic field on the morphology of the deposited Co films are discussed with respect to the different magnetically induced forces and the thereby-generated macro- and microconvections.

Experimental

The electrochemical investigations concerning the deposition of Co were carried out in two different types of cylindrical cells with different electrode geometries and electrode materials at 20°C. In one case the working electrode (WE) was a Cu disk with an area of 1 cm^2 embedded in epoxy resin (Fig. 1a). This electrode was placed horizontally or vertically in a thermostated cylindrical glass cell with an electrolyte volume of 200 mL described in detail in Ref. 23. Before each experiment the electrode was mechanically ground with emery paper grade 1000. In a second case the cell was a Teflon cylinder with a volume of 50 mL (Fig. 1b). The electrodes were slices cut from a Si wafer sputtered with a 100-nm Cu seedlayer for the investigation of the deposited film morphology or quartz slices with a Au layer for the electrochemical measurements. The area of the electrode was 1.55 cm^2. These electrodes were fixed with Viton O-rings and horizontally placed in the magnet. This construction leads to a wall around the electrode (wall electrode), which should influence the convection close to the surface.

In both cells the potentials were measured vs a sulfate reference electrode (SE) $Hg/Hg_2SO_4/1$ M H_2SO_4(+674 mV/SHE). Pt sheets were used as counter electrode (CE). The electrolyte was a 0.01 M $CoSO_4$ solution with addition of 0.1 M Na_2SO_4 as a supporting electrolyte. The pH value was adjusted with H_2SO_4 to pH 3. Cyclic voltammograms were recorded in the potential range between $E = -500$ mV to -1650 mV/SE with a scan rate of 20 mV s^{-1}.

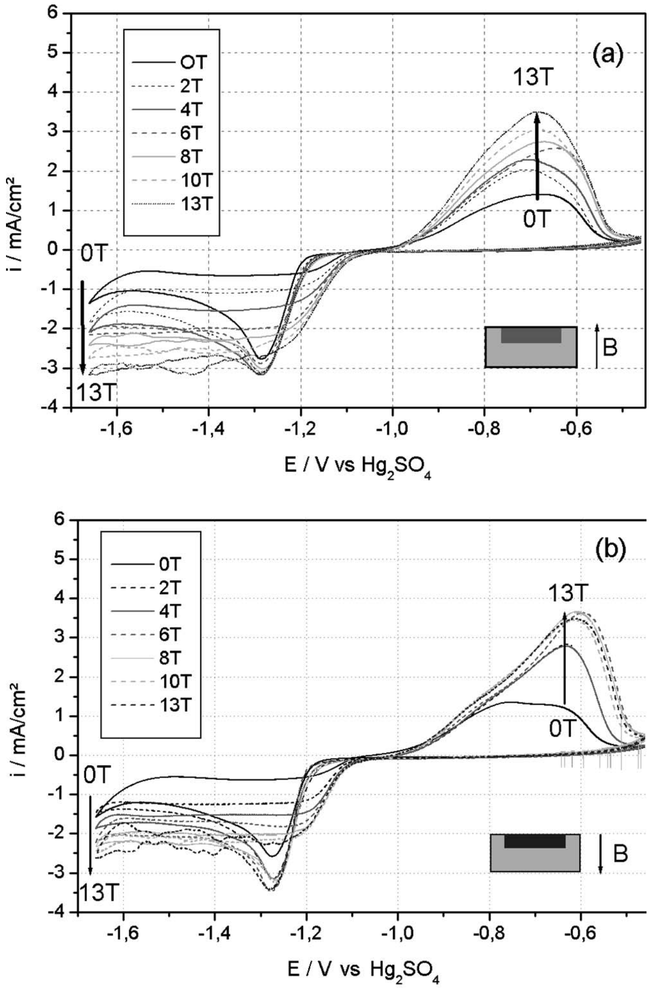

Figure 4. Cyclic voltammograms recorded in 0.01 M $CoSO_4$ + 0.1 M Na_2SO_4, pH 3, on flat embedded horizontal Cu electrodes for different magnetic flux densities; *B* is aligned (a) upward and (b) downward. dE/dt = 20 mV/s, 3rd scan.

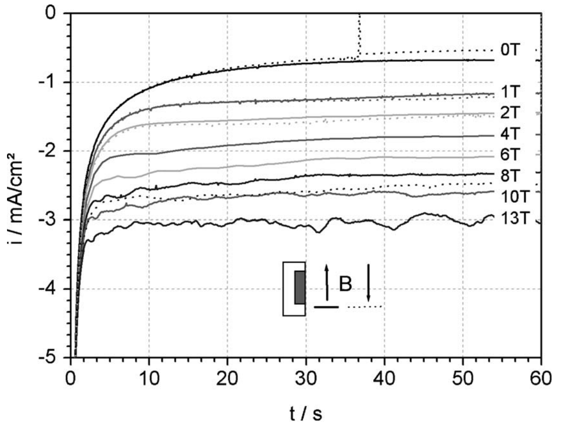

Figure 5. Limiting current density for the Co deposition in dependence on the magnetic flux density applied on the vertical flat embedded Cu electrode at $E = -1460$ mV/SE.

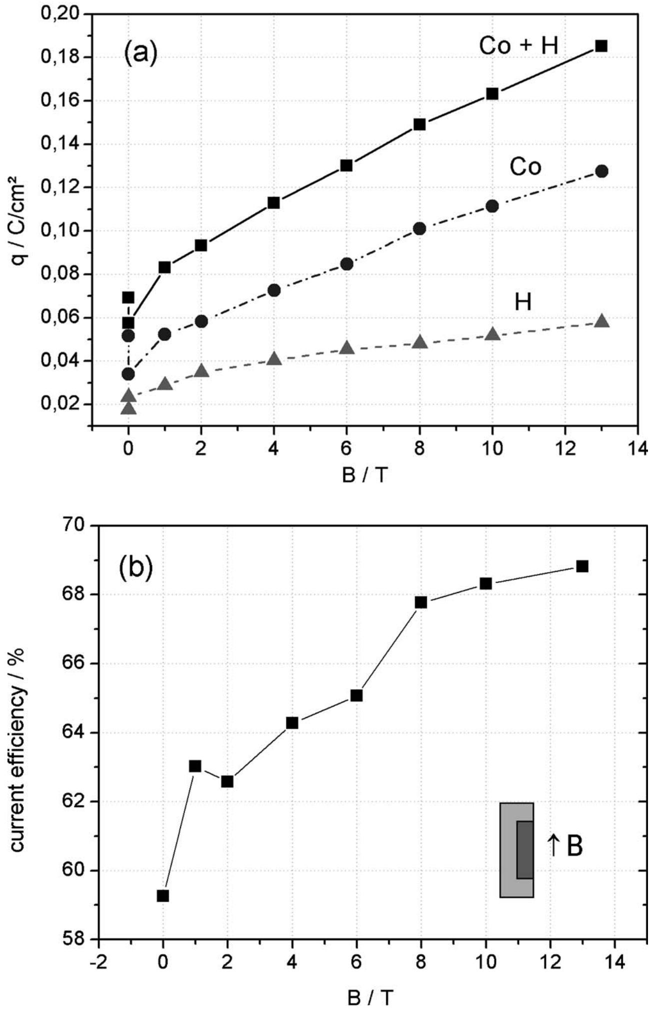

Figure 6. (a) Charge and (b) current efficiency in dependence on the magnetic flux density calculated from the deposition/dissolution measurements in Fig. 5.

From these scans the potential of $E = -1460$ mV/SE for deposition of Co and $E = -450$ mV/SE for dissolution of Co were selected for chronoamperometric measurements. The partial charges of Co deposition and hydrogen evolution as well as current efficiency for the Co deposition were calculated from these stripping experiments. The electrochemical investigations were carried out without and with superimposition of magnetic fields with a magnetic flux density up to 13 T. The magnetic field was generated in a resistive bore magnet of the Grenoble High Magnetic Field Laboratory (GHMFL) with a bore diameter of 130 mm and a high field homogeneity shown in Fig. 2.[36] The diagonal pattern indicates the distance of the electrode in the Teflon cell from the center of the magnet and the deviation in the magnetic flux density. For a magnetic field of 10 T the gradient $B(dB/dz)$ in the small Teflon cell is <1.7 T^2/m and therefore, is stated to be uniform across the geometry of the Teflon cell. The magnetic field gradient for the other cell amounts to maximum 20 T^2/m for a magnetic flux density of 10 T. Besides the measurements at constant magnetic flux densities, the magnetic field was linearly increased with a rate of 10 mT/s. Different configurations of the magnetic field to the electrode surface and thus to the electric field have been investigated, which are always highlighted in the figures. The morphology and roughness of the deposited Co layers were analyzed by atomic force microscopy (AFM) and the phase formation by X-ray diffraction (XRD) measurements.

Results

Cyclic voltammograms recorded in 0.01 M $CoSO_4$ on flat embedded horizontally and vertically aligned Cu electrodes with an upward and downward oriented magnetic field are shown in Fig. 3 and 4.

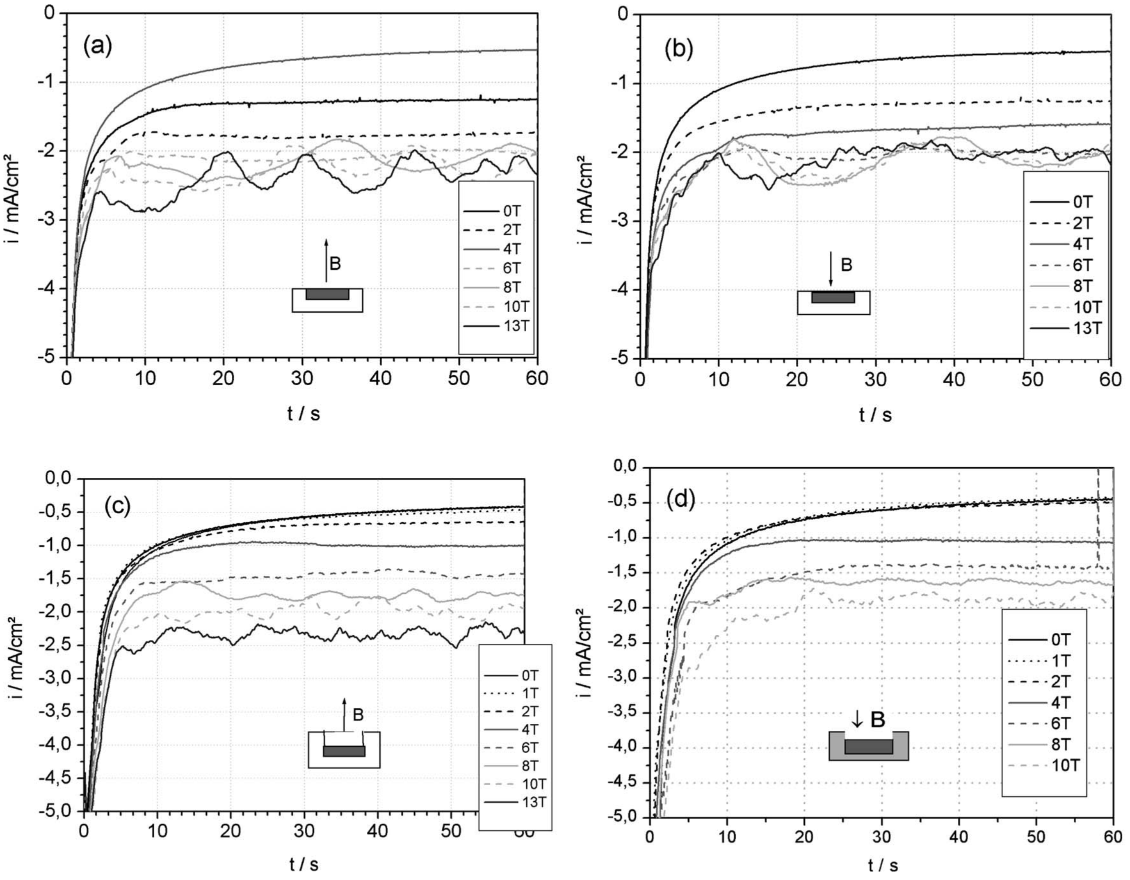

Figure 7. Limiting current density for the Co deposition at $E = -1460$ mV/SE in dependence on the magnetic flux density for two cell geometries and magnetic field orientations, (a, b) flat embedded electrodes and (c, d) wall electrodes.

The figures show clearly the differences in the cyclic voltammograms for the horizontally (Fig. 4) and vertically (Fig. 3) placed flat embedded Cu electrodes. The maximum limiting current density in dependence on the magnetic flux density is in the same order for both electrode alignments, but the Co dissolution peak is explicitly higher in the case of the vertically aligned electrode (Fig. 3), which indicates that a higher amount of Co was previously deposited. Oscillations in the current density are observed for high magnetic fields, especially in the case of the horizontally placed electrodes. It is obvious for the vertical electrode that the cathodic peak maximum shifts to more negative values with increasing magnetic field, whereas for the horizontal electrodes this maximum is more or less unaffected.

The effect of the magnetic field on the deposition behavior is established by the results of the chronoamperometric experiments shown in Fig. 5-7. The Co deposition potential of $E = -1460$ mV/SE was chosen from the cyclic voltammograms.

From stripping experiments the total and partial charges as well as the current efficiency with respect to the Co deposition were calculated. The limiting current density (Fig. 5) and the charge and current efficiency (Fig. 6a and b), respectively, reveal a strong increase with increasing magnetic flux density up to 13 T for the vertically aligned electrode and an upward oriented magnetic field. As seen in Fig. 6a, both reactions—the Co deposition and the H-ion reduction—increase in the same ratio. These results are in agreement with the results derived from the dynamic measurements (Fig. 3).

Figure 7a-d summarizes the change of the limiting current density for the Co deposition for two cell geometries of a horizontal placed electrode, i.e., the flat embedded electrode (a, b) and the electrode with a wall (c, d). The magnetic field is oriented up (a, c) or downward (b, d). For both geometries and field orientations the current density increases with increasing magnetic flux density. The change of the limiting current density is negligible for magnetic flux densities up to 2 T and it is small up to 6 T for the wall electrode. At high magnetic-flux densities a more pronounced increase occurs and the current density shows fluctuations. In contrast to that are the results obtained for flat embedded electrodes (a, b). The limiting current density increases by about a factor 2.5 already at magnetic flux densities of 2 T.

At high magnetic flux densities (>6 T) oscillations and no further increase of the limiting current density are observed. The current density oscillates with an amplitude of about 0.5 mA/cm^2. This behavior suggests that different magnetically induced driving forces overlap and determine the convection.

The partial charges and current efficiencies calculated on the basis of results shown in Fig. 7 are summarized in Fig. 8 and 9. They reveal very clearly the effect of the geometry of the cell. Altogether, the total charges (Co + H) as well as the partial charges for Co and for hydrogen-ion reduction increase with increasing magnetic field, but for the flat embedded electrodes it is obvious that the charge fraction of Co is always higher than the fraction of hydrogen. The increase of the slope of the total charges as well as of the partial charges is the highest for magnetic flux densities up to 4 T (Fig. 8a and b) and reaches a plateau at higher magnetic flux densities. Especially for the case of the downward oriented magnetic field (Fig. 8b), the charges and the limiting current densities keep constant at high magnetic flux densities. Besides that, the total charge and the partial charges of Co and hydrogen are higher in the upward oriented magnetic field than in the downward oriented magnetic field. This is in agreement with the cyclic voltammograms illustrated in

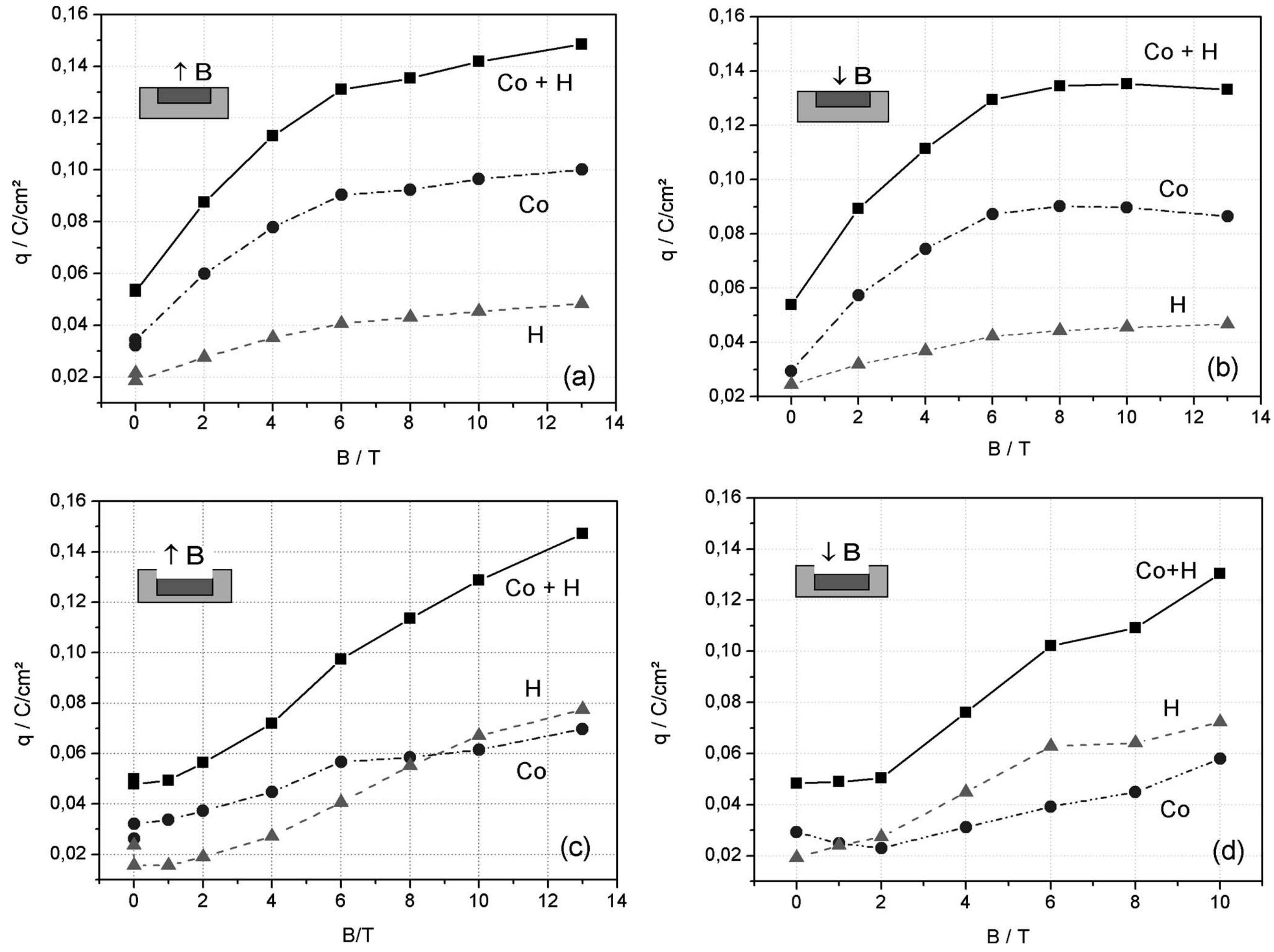

Figure 8. Total charge and partial charges of the reduction of Co and hydrogen ions in dependence on the magnetic flux densities and the cell geometry: (a, b) flat electrodes; (c, d) wall electrodes (c-the electrode was not 100% horizontal).

Fig. 3a and b and Fig. 4. For this flat cell geometry a strong rise in the current efficiency is observed from 0 to 2 T, but at high magnetic flux densities the current efficiency declines slightly (Fig. 8a and b). At high magnetic flux densities the Co deposition seems to be diminished at the expense of the hydrogen-ion reduction. This is also more pronounced for the case of the downward oriented magnetic field. The field-dependent behavior of the charges and current efficiencies is completely different for the wall electrodes shown in Fig. 8c and d, and Fig. 9c and d. A remarkable increase of the charges has not been observed below 2 T, but it strongly increases at magnetic flux densities above 4 T. For this cell geometry the hydrogen-ion reduction dominates the total reduction process, especially at high fields. The current efficiencies of Co decrease strongly for the wall electrodes at high fields (Fig. 9a and b).

Figure 10 establishes the findings for the horizontally and vertically placed flat electrodes during a continuous change of the magnetic flux density. For the vertically oriented electrode the limiting current density increases continuously with the magnetic field, whereas for the horizontal electrode the limiting current density initially decreases followed by a strong rise and some fluctuations occur.

The morphology of 50-nm-thick Co layers deposited by potentiostatic polarization at $E = -1450$ mV/SE on Si sheets with a 100-nm Cu seedlayer was investigated by AFM (Fig. 11) for vertical and horizontal wall electrodes and an upward-oriented magnetic field with flux densities up to 6 T. The deposition time was calculated from the Co charge in consideration of the current efficiency (Fig. 6a, 6b, 8c, and 9a). Magnetic fields oriented parallel to the electrode surface yield layers with randomly distributed spherical shaped grains (Fig. 11a-c). The shape of the grains and the roughness of the layer is similar for magnetic flux densities of 2 and 6 T. The morphology of the horizontal electrodes with the magnetic field oriented perpendicular to the surface is different. The surface is more rough with oval-formed grains (Fig. 11d-f). Figure 11e refers to microconvection on the surface.

Interestingly, the XRD patterns in Fig. 12 taken from the deposited Co layers of flat electrodes as well as the wall electrodes reveal that the structure is not changed in high magnetic fields oriented parallel or perpendicular to the surface as compared to low magnetic fields discussed in Ref. 37 and 38. All Co layers show reflexes at the same angle between the face-centered cubic (fcc) and hexagonal close-packed (hcp) lattice structures of Co.

Discussion

The Co deposition from the 0.01 $CoSO_4$ electrolyte at pH 3 is always accompanied by the reduction of hydrogen ions. For the chosen experimental conditions both reactions are mass controlled in the potential range of -1200 to -1500 mV/SE, as it has been shown in earlier investigations.[21-23] Therefore, in order to discuss the results both reactions have to be considered.

B parallel to the surface.— For the classical configuration, with a magnetic field applied parallel to the electrode surface it is expected that both partial reactions should be affected by the field. As

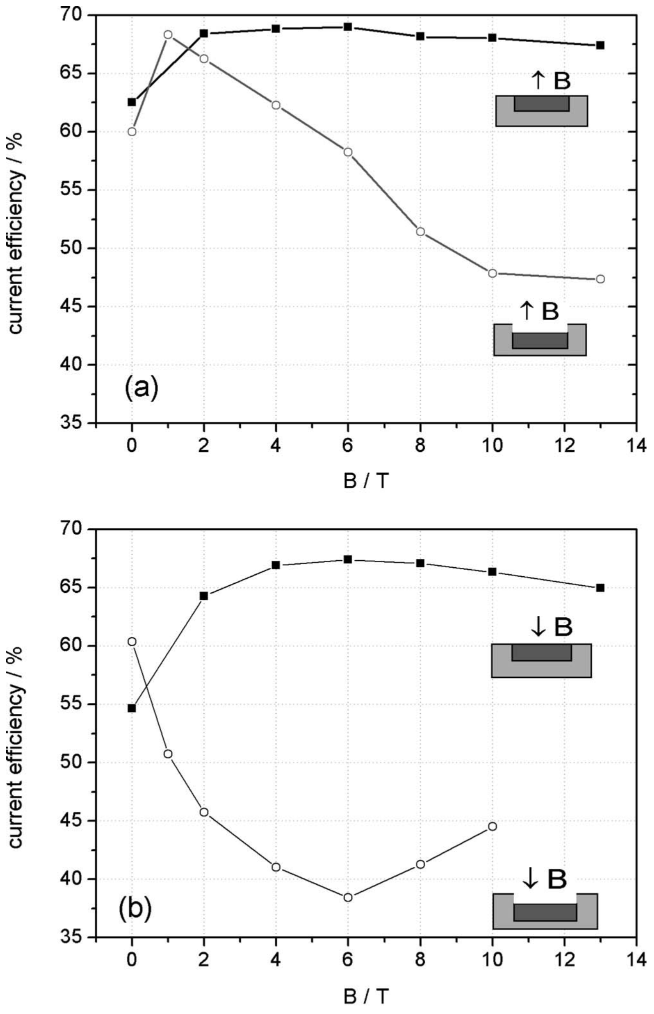

Figure 9. Current efficiency for the Co deposition in dependence on the magnetic flux densities and the cell geometry: (a) upward oriented magnetic field and (b) downward oriented magnetic field.

has been shown in Fig. 3, 5, 6, and 10, the limiting current density increases with the magnetic flux density, which is only due to the Lorentz force and thus convection generated, but a significant rise does not start before the magnetic flux density exceeds 250 mT (Fig. 10). This corresponds to a Lorentz force of nearly 2 $\mathrm{N/m^3}$, which is in agreement with the result for the Cu deposition obtained in earlier experiments under the same conditions.[23] The threshold of about 2 $\mathrm{N/m^3}$ has to be exceeded to overcome the natural convection, which induces a weak upward flow of the electrolyte to compensate the depletion of ions. The vertical laminar natural convection is overlapped by a horizontal tangential flow in the vicinity of the surface. This flow is directed clockwise or counterclockwise depending on the orientation of the magnetic field, i.e., if it is aligned upward or downward. Figure 6a shows that both reactions, the $\mathrm{Co^{2+}}$ and the hydrogen-ion reduction, increase but the latter to a less extent, and Fig. 6b reveals that the Co efficiency increases too. An increasing hydrogen-ion reduction was also proved for magnetic field of 1 T.[37] It has been shown in Ref. 21 and 22 that in an external field of 1 T the layers are more homogeneous and without defects caused by hydrogen bubbles that are removed faster by the forced convection. An additional convection might be expected due to the take-off of hydrogen bubbles, which are formed during polarization. However, this contribution should be negligible because the partial charge after 60 s polarization is only between 20 and 50 $\mathrm{mC/cm^2}$. This corresponds to a hydrogen volume of 2–5 $\mathrm{mm^3}$, which is formed on a area of 1 $\mathrm{cm^2}$ during a period of 60 s. A significant convective contribution is improbable. Besides that the threshold of the magnetic field for generating convection is the same for the Co deposition and for the Cu deposition, during which no hydrogen ions are reduced.[23] As generally known, convection diminishes the diffusion layer thickness. Taking into account that the diffusion coefficient is unaffected by an external magnetic field,[1] the diffusion layer thickness δ can be calculated by the relation $i_{\mathrm{lim}} = nFDc_\infty/\delta$. The diffusion coefficient was determined to 8.8×10^{-6} $\mathrm{cm^2/s}$ by the Cottrell equation from the current–time transient recorded without magnetic field. The current efficiency is only about 60% at $B = 0$ T and 70% at $B = 13$ T. Therefore, the calculated diffusion coefficient has to be regarded as a guiding value. Literature data for metal ions are in the same order of magnitude, i.e., about 10^{-5} $\mathrm{cm^2/s}$. The decrease of the diffusion layer thickness in dependence on the magnetic field is shown in a double-log plot in Fig. 13. The circles represent the data calculated from the potentiostatic measurements (Fig. 5), whereas the line is calculated from the curve in Fig. 10 recorded with $dB/dt = 10$ mT/s. Both results are consistent. At 2 T the diffusion layer is reduced to one half of the original value at 0 T and is only about one quarter at 13 T.

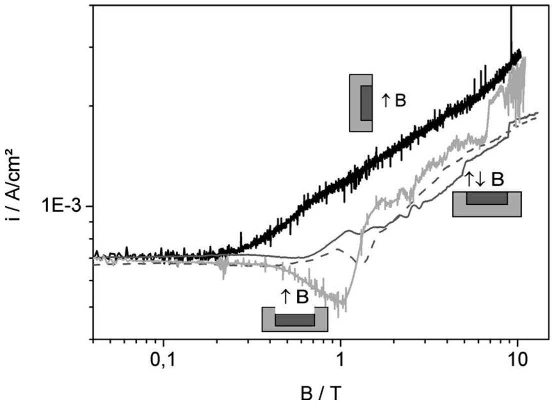

Figure 10. Limiting current density for different cell and magnetic field orientation recorded during continuous change of the magnetic flux density, $dB/dt = 10$ mT/s.

The slope of the double-log plot i_{lim} (Fig. 10) and δ (Fig. 13), respectively, vs B is a useful tool to compare the results with published data and especially to evaluate the generated convection. The curves of the flat embedded vertical electrode are nearly linear after exceeding the threshold of B. Therefore, they fit to the expected and proved progression. The exponents for B and the diffusion layer are $1/3$ and $-1/3$, respectively.[7-11]

Different considerations were made to describe the magnetic-field-induced convection under hydrodynamic conditions.[7,8,13,14] The mathematical analysis of the convective diffusion equation and Navier–Stokes equation yielded the semiquantitative relations to describe the laminar or rotating flow of planar hydrodynamic electrodes in general[6] (see Eq. 1 and 2), but only some numerical simulations are published to describe the concentration and velocity gradient in the vicinity of the electrode superimposed with parallel magnetic fields. These calculations are not transferable to other experimental setups. In order to estimate the laminar flow, the simplified approach of Eq. 1 was applied for the flat embedded disk electrode. A Lorentz force of about 2 $\mathrm{N/m^2}$ is required to induce a convection and to counteract the natural convection, as was discussed above and also in Ref. 23. From this threshold the velocity increases continuously with increasing magnetic flux density and the slope of the double-log plot corresponds to B^b with $b = 0.74$ (Fig. 14). Therefore, the slope is higher than the expected $b = 2/3$ and the laminar flow is overestimated by this simple approach. One reason is that for the estimation of the laminar flow the overall current density was used. It has to be considered that the electrochemical process consists of two reactions, the Co deposition and hydrogen-

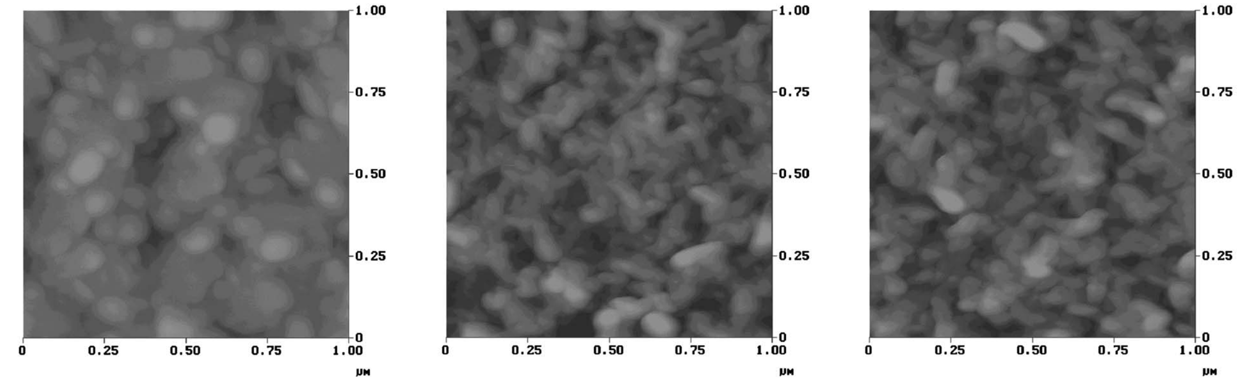

a-0T (z=100nm) RMS:6nm b-2T (z=100nm) RMS:11nm c-6T (z=100nm) RMS:11nm

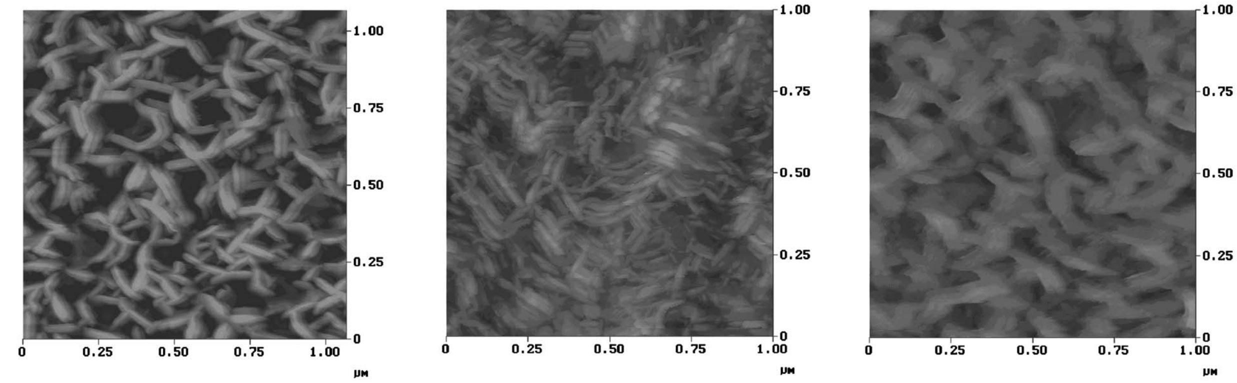

d-2T (z=100nm) RMS:19nm e-4T (z=100nm) RMS:10nm f-6T (z=200nm) RMS: 18nm

Figure 11. AFM images showing the morphology and roughness of 50-nm-thick Co layers deposited on Cu: (a–c) vertical electrode and (d–f) horizontal wall electrode.

ion reduction, which contribute differently to the convection due to the different diffusion coefficients, different concentrations, and different thicknesses of the diffusion layer. Therefore, overlapping convective effects have to be taken into account, whereby the flux of the Co ions should determine the resulting convection. Besides the laminar convection, a rotating flow at the edge of the electrode due to the electric field lines that are not parallel should have a small, but additional influence. In summary, it has to be concluded that the investigated system obeys the known and well-established theory of MHD in magnetic fields with high magnetic flux densities up to 13 T aligned parallel to the electrode surface of flat embedded macroscopic disk electrodes.

B perpendicular to the surface.— In general, convective effects have been controversially discussed for the case of magnetic fields oriented perpendicular to the electrode surface. Investigations on microdisk electrodes have shown that the field gradient force can act in the volume electrolyte as well as in the vicinity of the electrode inside the electrochemical diffusion layer and induces microfluctuations on the surface, thus moving paramagnetic/diamagnetic ions toward or away from the surface.[18-20,24,25,29-35] Recently, it has been shown by us that different magnetically induced forces can induce a convection also on macroscopic electrodes and influence deposition behavior.[21-23] The results of the cyclic voltammograms (Fig. 4), the chronoamperometric measurements (Fig. 7), the calculated partial charges for the two reactions (Fig. 8), and the current efficiency for the Co deposition (Fig. 9) reveal that the magnetic field affects the deposition behavior significantly and that the cell/electrode geometry is an important factor. For both electrode geometries, i.e., the flat disk electrode and the wall electrode, i_{lim} increases with increasing magnetic flux density. The maximum current density at 13 T is comparable for both types of horizontal electrode and is only slightly lower in comparison with that of the vertical electrode. Oscillations are observed for high flux densities, especially for the flat electrodes. The main difference between the electrode types has been detected in the current efficiency of the Co^{2+} reduction. It increases for vertical flat electrodes (see above), remains constant or increases only slightly for horizontal flat electrodes, and decreases for the horizontal wall electrodes with increasing magnetic flux density, in upward as well as downward aligned magnetic fields (Fig. 9). The same conclusions are drawn from the cyclic voltammograms. The scans in Fig. 4 reveal that the onset potential of the decrease of cathodic current density and the peak maximum are equal for all magnetic flux densities for the horizontal flat electrode, whereas a shift to more negative values is observed for the vertical electrode. These findings are attributed to a preferred reduction of hydrogen ions, which is confirmed by the smaller dissolution peak of Co. Therefore, the results cannot be discussed only by MHD effects. Other magnetically induced forces have to be taken into account to understand the changed deposition behavior. In contrary to the investigations in Ref. 18-20 and 29-34, the magnetic field of the resistive magnet in the GHMFL is very homogeneous. The field gradient of the magnet itself in the small cell with the wall electrode is negligible, as can be seen from Fig. 2. The same constant magnetic field can be assumed for the large cell in front of the electrode. Therefore, an effect of the magnetic field gradient force induced by the magnet is improbable and is not discussed. During the deposition the formed Co layer is ferromagnetic and could contribute to an additional field gradient in the close vicinity of the surface, but in

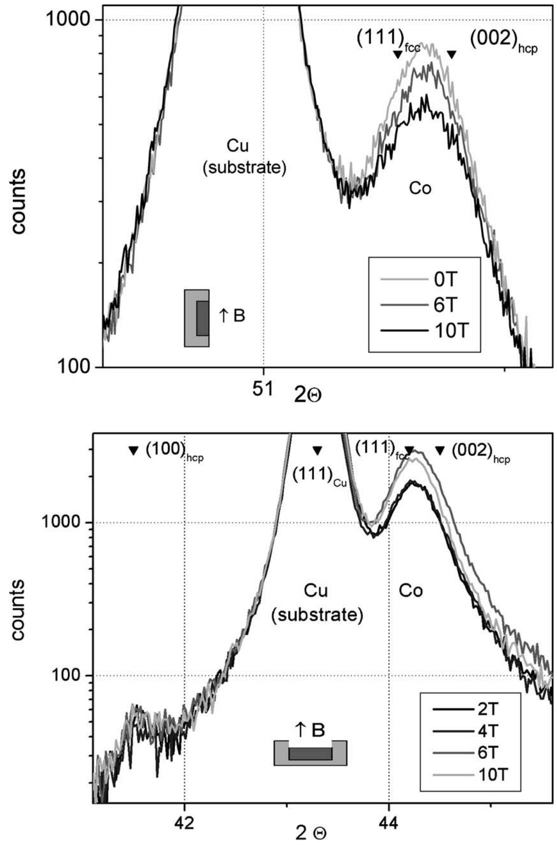

Figure 12. XRD pattern of 50-nm Co layers deposited on vertically placed flat Cu electrodes, (a) Co (Kα) and horizontally placed wall electrodes, (b) Cu (Kα).

the high external magnetic fields the formed layer is in a single domain state and a field gradient should be marginal. Besides that a potential magnetic field gradient due to the magnetization of the formed thin Co layer should lead to an increased Co deposition, because the paramagnetic Co^{2+} ions should move in the direction of the field gradient, which is always oriented in the direction of the highest flux density (Eq. 4). The contribution of a magnetic field gradient to the general electrochemical behavior seems to be negligible, because the oscillation at high fields (Fig. 7a and b) and the decrease of the current density as well as the decrease of the deposited metal already at low fields (Fig. 10) were also observed for the deposition of nonmagnetic Cu, as reported in Ref. 22. For a horizontal electrode with the magnetic field perpendicular to the surface, a rotating flow can be expected due to the nonparallel field lines at the edge. The estimated rotating flow from Eq. 2 is shown in Fig. 15. To simplify, it was assumed that the total current density and therefore the sum of the moved electroactive species contribute to the rotational flow. The rotation for the flat electrode is fast at low fields and merges in an apparently stable state with increasing magnetic field. Because of the wall of the other electrode type and the more parallel electric field lines, the rotational flow is negligible for low fields but increases with increasing magnetic field and attains the same value at 13 T as for the flat electrode. The assumption of a stable rotation is not really true, as can be seen from the oscillating behavior of i_{lim} in Fig. 7. The mean circumferential velocity at the edge of the electrodes is therefore lower than the laminar flow in front of the vertical electrode. These results and the fact that the current efficiency for the Co deposition decreases with increasing magnetic flux density allow the prediction to be made that other forces superimpose the behavior and act opposite.

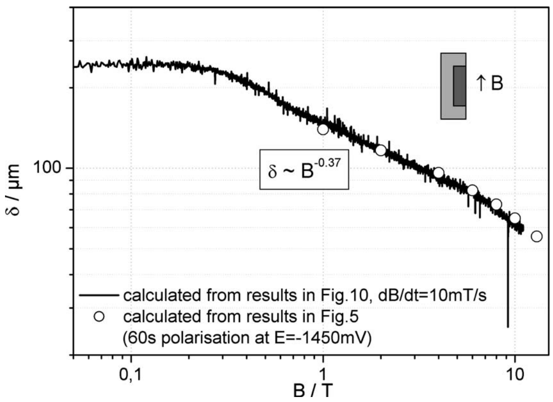

Figure 13. Evolution of the diffusion layer thickness at the surface of a vertical flat Cu disk electrode with an increasing upward aligned magnetic field.

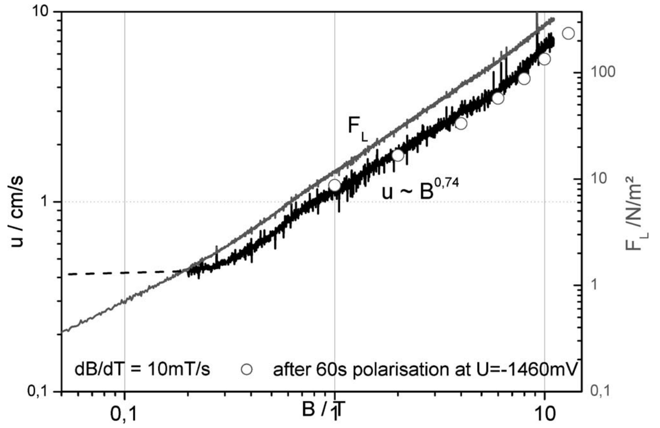

Figure 14. Lorentz force (F_L) and estimated velocity of the induced laminar flow (u) in dependence on the magnetic field of the vertical flat Cu disk electrode, upward aligned B, $dB/dt = 10$ mT/s.

It has been discussed that for the investigated electrochemical system and the used experimental facility the field gradient force is negligible. Suiyama et al.[35] predict a convective diffusion layer with a self-organizing process for adjusting the diffusion layer thickness wherein magnetoconvection drives the electroactive species. Numerous minute convection cells are formed due to the magnetic field gradient and the gradient of concentration. Because the magnetic field gradient is negligible in our case, only a driving force caused by the gradient of the magnetic susceptibility can determine the magnetoconvection. This paramagnetic gradient force $F_{\nabla p}$ (Eq. 5) is aligned perpendicular to the surface due to the same direction of the concentration gradient. The volume magnetic susceptibility χ of the paramagnetic Co ion is 10^{-8} m^3/mol, whereas the hydrogen ions are nonmagnetic and anions and molecular hydrogen are diamagnetic with a weak magnetic susceptibility. These species will not contribute to a remarkable weakening of the flow of electrolyte close to the surface. Because the volume magnetic susceptibility of the Co ions has a positive algebraic sign, the ions were moved away from the electrode in the direction of the concentration gradient, that means opposite to the driving force of the diffusion. Therefore, caused by the magnetic properties of the Co ions, a paramagnetic gradient force drives a convection inside the diffusion layer. The orientation of the magnetic field should be irrelevant because the magnetic flux density is B^2 in the formula (Eq. 5).

Derived from the relations discussed in Ref. 35, the convective diffusion layer in uniform magnetic fields can calculated by

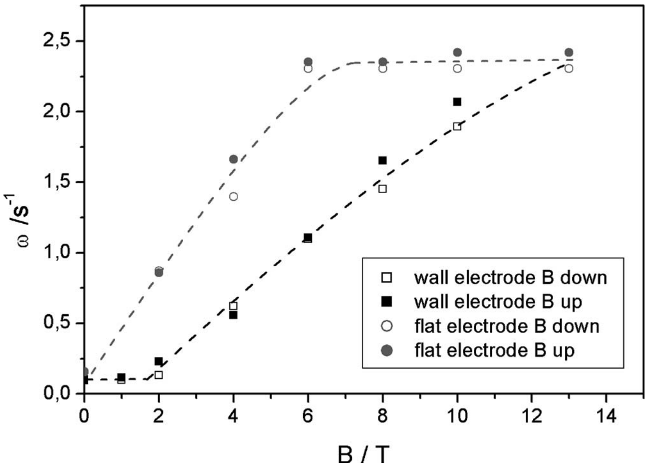

Figure 15. Estimated rotating flow (ω) in dependence on the magnetic field of the horizontal flat electrodes and wall electrodes (Eq. 2). The dashed lines are guides for the eyes.

$$\delta_c = 10.32(2\mu_0 D\eta/B^2\chi\ \nabla\ c)^{1/3} \qquad [7]$$

Figure 16 shows the theoretical change of δ_c vs the magnetic field without consideration of the rotational flow and the resultant paramagnetic gradient force. Comparable to the parallel magnetic field configuration, the thickness of the diffusion layer decreases and reaches a similar value of about 50 μm (compare Fig. 13) at a magnetic flux density of 13 T. Hence, the resulting force $F_{\nabla p}$ is 1.4×10^6 N/m^3. The curves of the current density for Co in Fig. 17 as well as the total and partial charges in Fig. 6 and 8 indicate no difference between the partial current density of Co-ion reduction for flat embedded vertical and horizontal electrodes. The result of this might be that the convection is determined in principle by the same origin, the MHD effect, caused by the laminar flow or the rotating flow. This conclusion is supported by the slope of the double-log plot in which b is 0.37 for the flat embedded electrodes up to 6 T (Fig. 10 and 17). This laminar or rotating flow is driven by a Lorentz force of maximum 150 N/m^3. The expected convection in dependence on the magnetic flux density is schematically drawn for the two types of horizontal electrodes in Fig. 18. For low magnetic flux densities, after exceeding a threshold the deposition is dominated by the rotating convection due to the Lorentz force for the flat electrodes. At higher magnetic fields, the Co deposition is suppressed for this electrode type caused by the paramagnetic gradient force that repulses the Co ions and the molecular hydrogen away from the electrode. For the wall electrode the partial current of Co decreases slightly up to 1 T, as was discussed in Ref. 22, and increases at higher magnetic flux densities with a slope of $b = 0.78$, whereby the maximum partial current of the flat electrode is not achieved. This slope is consistent with the deviation of Eq. 8,[34] which claims a $B^{2/3}$ dependency for magnetic and concentration gradient forces

$$i = 0.0969nFc_\infty D\left(\frac{1}{2\mu_0 D\eta}\right)^{1/3}\left(\frac{\partial\chi}{\partial c}\right)^{1/3}|\Delta c|^{4/3}B^{2/3} \qquad [8]$$

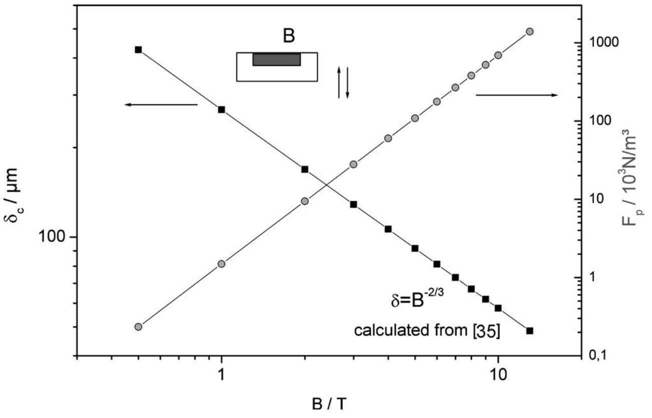

Figure 16. Calculated change of the convective diffusion layer thickness δ_c (Ref. 35) and the paramagnetic gradient force F_p, respectively, vs the magnetic flux density.

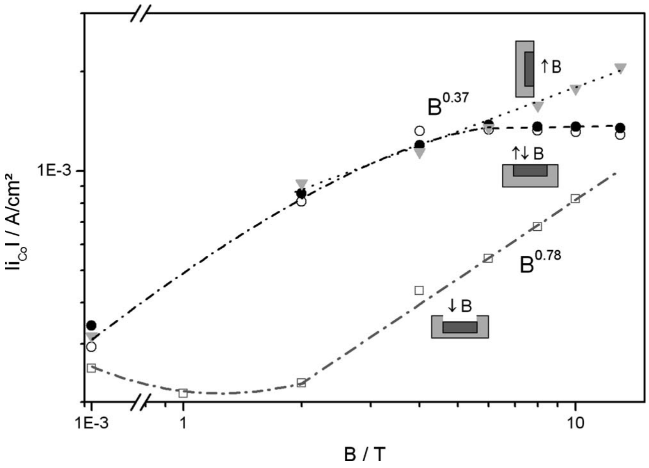

Figure 17. Partial current densities of the Co ion reduction in dependence on the magnetic field for various electrode geometries and orientations.

The current efficiency (Fig. 9) reveals a pronounced reduction of hydrogen ions favored by the fast removal of the reduced hydrogen molecules from the electrode surface. The rotation induced by the total flow of the electroactive species dominates the electrochemical behavior on the flat embedded electrode for magnetic flux densities up to 6 T caused by the predominantly higher amount of nonparallel electric field lines at the edge of the disk electrode, in comparison to the alignment at the wall electrode. At high fields the Co deposition is suppressed by the strong paramagnetic gradient force of about 10^6 N/m^3. With decreasing diffusion layer thickness and increasing concentration gradient, the probability for the influence of the paramagnetic gradient force should be more dominant and more determined for the deposition behavior. The oscillations in the current density reveal the effect of overlapping forces (Fig. 5). For the wall electrodes the rotation is low at low magnetic flux densities. Therefore this paramagnetic gradient force has a predominant effect already at low magnetic flux densities. Higher fields induce also at the wall a rotational flow which counteracts the paramagnetic force. It is discussed in Ref. 18-20, 34, and 35 that gradients of the magnetic flux density and susceptibility together with charge fluctuations lead to microconvections and vortexes directly at the surface. The AFM investigations show clearly differences between the Co layers deposited on vertically and horizontally arranged electrodes. Whereas for the vertical electrode the spherical shaped grains are randomly distributed, the morphology of the deposits on the horizontal electrode shows an inhomogeneous structure. An evolution of this morphology can be due to the proposed magnetoconvection, but this is only caused by the gradient of the concentration and volume magnetic susceptibility and not by the gradient of the magnetic flux density. Differences in the morphology in the cross section of the deposits were observed but not systematically investigated.

Conclusion

The effect of vertically oriented, uniform high magnetic fields on the electrodeposition of Co has been investigated in dependence on the cell and electrode geometry as well as the orientation and

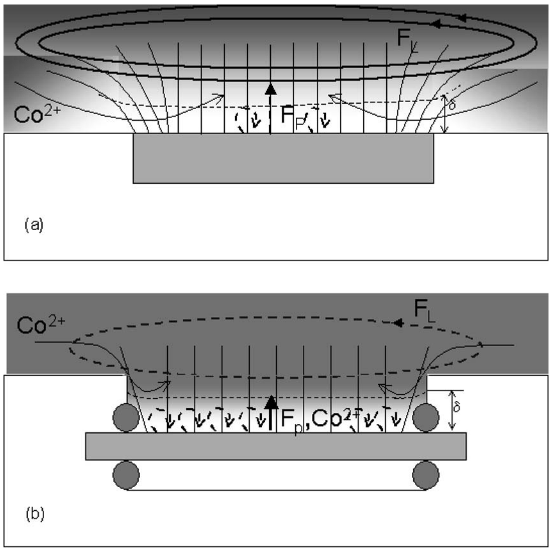

Figure 18. Scheme of the expected convection and of the contribution of the acting forces for the two types of horizontal electrodes.

$B < 1T \quad F_p > F_L \quad i_{lim}\downarrow$ (Fig.10) $\quad B < 1T \quad F_p > F_L \quad i_{lim}\downarrow, i_{Co}\downarrow$

$B > 1T \quad F_p < F_L \quad i_{lim}\uparrow\uparrow, i_{Co}\uparrow\uparrow \quad B > 2T \quad F_p > F_L \quad i_{lim}\uparrow\uparrow, i_{Co}(\uparrow)$

$B > 6T \quad F_p \cong F_L \quad i_{lim}, i_{Co}$ const. $\quad B > 6T \quad F_p < F_L \quad i_{lim}\uparrow, i_{Co}(\uparrow)$

strength of the magnetic flux density by means of cyclic voltammetry, chronoamperometry, AFM, and XRD measurements.

For all electrode geometries and orientations of the magnetic field relative to the electrode surface an increase of the limiting current density i_{lim} with increasing magnetic flux density has been observed. Magnetic fields aligned parallel to vertical flat electrodes increase the current efficiency of the Co-ion reduction with increasing magnetic flux densities due to the classical MHD effect generated by the Lorentz force. The well-known relation $i_{lim} \propto B^{1/3}$ has been established also for high magnetic flux densities. The deposited layer morphology exhibits randomly distributed grains of spherical shapes.

The electrochemical behavior on horizontal electrodes with magnetic fields arranged perpendicular to the electrode surface is strongly dependent on the electrode geometry. The current efficiency of the Co deposition increases for low magnetic flux densities and keeps constant for high magnetic fields, whereas for wall electrodes the current efficiency decreases already strongly for low magnetic fields. These results are caused by overlapping effects of two types of convections in the vicinity of the electrode. Rotational MHD effects due to nonparallel electric field lines at the edge of the electrode dominate the behavior on flat embedded disk electrodes. At high fields the paramagnetic gradient forces diminish the discharging of the Co ions. This force determines the deposition on wall electrodes. Due to the gradient of the paramagnetic susceptibility the Co ions are repelled from the electrode surface. This leads to micro-magnetoconvection within the diffusion layer and to an inhomogeneous morphology with a circle-like pattern. Only at high fields macro-MHD-convection influences the deposition. It could be shown that micro-magnetoconvection is not only bounded to magnetic field gradients but also to gradients of concentration and magnetic susceptibility, respectively.

Acknowledgment

The measurements were carried out in the Grenoble High Magnetic Field Laboratory. The German Research Council (DFG) is gratefully acknowledged for support within the framework of the SFB 609.

The Leibniz-Institute for Solid State and Materials Research assisted in meeting the publication costs of this article.

References

1. T. Z. Fahidy, *Electrochim. Acta*, **18**, 607 (1973).
2. T. Z. Fahidy, *Prog. Surf. Sci.*, **68**, 155 (2001).
3. R. A. Tacken and L. J. J. Janssen, *J. Appl. Electrochem.*, **25**, 1 (1995).
4. O. Devos, O. Aaboubi, J.-P. Chopart, E. Merienne, A. Olivier, and J. Amblard, *J. Electrochem. Soc.*, **145**, 4135 (1998).
5. K. Msellak, J.-P. Chopart, O. Jbara, O. Aaboubi, and J. Amblard, *J. Magn. Magn. Mater.*, **281**, 295 (2004).
6. M. A. Brett and A. M. O. Brett, *Electrochemistry Principles, Methods, and Applications*, p. 152, Oxford University Press, New York (1998).
7. R. Aogaki, K. Fueki, and T. Mukaibo, *Denki Kagaku oyobi Kogyo Butsuri Kagaku*, **43**, 504 (1975).
8. R. Aogaki, K. Fueki, and T. Mukaibo, *Denki Kagaku oyobi Kogyo Butsuri Kagaku*, **43**, 509 (1975).
9. O. Aaboubi, J.-P. Chopart, J. Douglade, A. Olivier, C. Gabrielli, and B. Tribollet, *J. Electrochem. Soc.*, **137**, 1796 (1990).
10. J. P. Chopart, O. Aoboubi, E. Merienne, A. Olivier, and J. Amblard, *Energy Convers. Manage.*, **43**, 365 (2002).
11. A. Olivier, J. P. Chopart, J. Douglas, and C. Gabrielli, *J. Electroanal. Chem. Interfacial Electrochem.*, **217**, 443 (1987).
12. G. B. Ngo Boum and A. Alemany, *Electrochim. Acta*, **44**, 1749 (1999).
13. N. Leventis and X. Gao, *J. Phys. Chem. B*, **103**, 5832 (1999).
14. N. Leventis, M. Chen, X. Gao, M. Canalas, and P. Zhang, *J. Phys. Chem. B*, **102**, 3512 (1998).
15. P. Fricoteaux, B. Jonvel, and J.-P. Chopart, *J. Phys. Chem. B*, **107**, 9459 (2003).
16. A. Olivier, J.-P. Chopart, J. Amblard, E. Merienne, and O. Aaboubi, *ACH-Models Chem.*, **137**, 213 (2000).
17. J.-P. Chopart, A. Olivier, E. Merienne, J. Amblard, and O. Aaboubi, *Electrochem. Solid-State Lett.*, **1**, 139 (1998).
18. R. Aogaki, *Magnetohydrodynamics*, **39**, 453 (2003).
19. R. Aogaki, *Magnetohydrodynamics*, **37**, 143 (2001).
20. R. Aogaki, A. Tadano, and K. Shinohara, *Transfer Phenomena in Magnetohydrodynamic and Electroconducting Flows*, A. Alemany et al., Editors, p. 169, Kluwer Academic Publishers, Norwell, MA (1999).
21. A. Krause, M. Uhlemann, A. Gebert, and L. Schultz, *Electrochim. Acta*, **49**, 4127 (2004).
22. K. L. Rabah, J. P. Chopart, H. Schlörb, S. Saulnier, A. Aaboubi, M. Uhlemann, D. Elmi, and J. Amblard, *J. Electroanal. Chem.*, **571**, 85 (2004).
23. M. Uhlemann, H. Schlörb, K. Msellak, and J. P. Chopart, *J. Electrochem. Soc.*, **151**, C598 (2004).
24. R. N. O'Brien and K. S. V. Santhanam, *J. Appl. Electrochem.*, **27**, 573 (1997).
25. R. N. O'Brien and K. S. V. Santhanam, *J. Appl. Electrochem.*, **20**, 427 (1990).
26. M. Waskaas and Y. I. Kharkats, *J. Phys. Chem. B*, **103**, 4876 (1999).
27. M. Waskaas, *J. Phys. Chem.*, **97**, 6470 (1993).
28. A. Bund, S. Köhler, H. H. Kühnlein, and W. Plieth, *Electrochim. Acta*, **49**, 147 (2003).
29. S. R. Ragsdale, K. M. Grant, and H. S. White, *J. Am. Chem. Soc.*, **120**, 13461 (1998).
30. K. M. Grant, J. W. Hemmert, and H. S. White, *J. Electroanal. Chem.*, **500**, 95 (2001).
31. K. M. Grant, J. W. Hemmert, and H. S. White, *Electrochem. Commun.*, **1**, 319 (1999).
32. M. D. Pullins, K. M. Grant, and H. S. White, *J. Phys. Chem. B*, **105**, 8989 (2001).
33. G. Hinds, J. M. D. Coey, and M. E. G. Lyons, *Electrochem. Commun.* **3**, 213 (2001).
34. A. Sugiyama, M. Hashiride, R. Morimoto, Y. Nagai, and R. Aogaki, *Electrochim. Acta*, **49**, 5115 (2004).
35. A. Sugiyama, S. Morisaki, and R. Aogaki, *Jpn. J. Appl. Phys., Part 1*, **42**, 322 (2003).
36. http://ghmfl.grenoble.cnrs.fr
37. M. Uhlemann, A. Krause, and A. Gebert, *J. Electroanal. Chem.*, **577**, 14 (2005).
38. A. Krause, C. Hamann, M. Uhlemann, and A. Gebert, *J. Magn. Magn. Mater.*, **290–291**, 261 (2005).